Structural Engineering and Mechanics, *Vol. 70, No. 3 (2019) 311-324*
DOI: https://doi.org/10.12989/sem.2019.70.3.311

Coupling effects between wind and train transit induced fatigue damage in suspension bridges

Francesco Petrini*[1a], Pierluigi Olmati[2] and Franco Bontempi[1]

[1]*Department of Structural and Geotechnical Engineering, Sapienza University of Rome, Via Eudossiana 18, Rome, Italy*
[2]*Taisei Corporation, Shinjuku Center Building, Nishi Shinjuku 1-25-1, Tokyo, Japan*

(Received August 24, 2018, Revised February 20, 2019, Accepted February 24, 2019)

Abstract. Long-span steel suspension bridges develop significant vibrations under the effect of external time-variable loadings because their slenderness. This causes significant stresses variations that could induce fatigue problems in critical components of the bridge. The research outcome presented in this paper includes a fatigue analysis of a long suspension bridge with 3300 meters central suspended span under wind action and train transit. Special focus is made on the counterintuitive interaction effects between train and wind loads in terms of fatigue damage accumulation in the hanger ropes. In fact the coupling of the two actions is shown to have positive effects for some hangers in terms of damage accumulation. Fatigue damage is evaluated using a linear accumulation model (Palmgren-Miner rule), analyses are carried out in time domain by a three-dimensional non-linear finite element model of the bridge. Rational explanation regarding the above-mentioned counterintuitive behavior is given on the basis of the stress time histories obtained for pertinent hangers under the effects of wind and train as acting separately or simultaneously. The interaction between wind and train traffic loads can be critical for a some hanger ropes therefore interaction phenomena within loads should be considered in the design.

Keywords: suspension bridges; fatigue analysis; wind-train interaction; damage accumulation; non-linearity

1. Introduction

Long-span suspension bridges are one steel structure typology with great proneness to vibrations-induced fatigue problems. Reasons of this weakness are related to both structural properties and nature of loadings. Furthermore, typical loadings such as wind forces and railway or roadway traffic have cyclic behavior which can affect the dynamic response causing random vibrations and critical stresses. Therefore, fatigue assessment is a must for a performance based design of such a kind of structural systems (Gimsing and Georgakis 2012, Barbato *et al.* 2014, Sgambi *et al.* 2014), also because in extreme cases fatigue failures can lead to disastrous consequences like progressive collapse (Brando *et al.* 2012, Olmati and Giuliani 2013, Olmati *et al.* 2013). Many researches have been carried out on fatigue problems for long-span suspension bridge focusing principally on welded connections along the deck (Chan *et al.* 2003, Chan *et al.* 2005). As well-known, connections are typical hot-spots for fatigue assessment because welds (such as holes or notches) induce an inhomogeneous stress distribution where high stress peaks could reach critical values thus cracks may generate. Also, if usually they are built by avoiding welds, a specific fatigue analysis must be performed on the connections between the deck and the suspension system of the bridge (e.g., hanger ropes) which experiences high stress variations during the lifetime under wind action and railway traffic and which in the past exhibited unexpected fatigue cracks in existing bridges (Klinger *et al.* 2014, Sun *et al.* 2017, Zhong *et al.* 2018). In particular, the importance of wind-induced fatigue increases with the length of the bridge (Xu *et al.* 2009), with hanger ropes being or not critical components for fatigue strength also depending on their location along of the deck (Liu *et al.* 2017). On the other hand, train and vehicles-induced fatigue problems are recognized as a common issue for hangers (Ye *et al.* 2014).

In the problem of fatigue assessment of steel structures under multiple types of actions, particular attention must be devoted to the interaction mechanisms between different loads (Manenti and Petrini 2010), such as those due to wind and train transit in case of long span suspension bridges (Petrini and Bontempi 2011). This problem has been partially studied in literature; in detail, Chen *et al.* (2011) proposed a framework for fatigue analysis of a long-span suspension bridge under multiple loading by integrating computer simulation with structural health monitoring (SHM) system; they highlighted the necessity to take into account the combined effect of multiple loading scenarios for the correct evaluation of the fatigue life of a complex structural system like a long-span suspension bridge. Zhang *et al.* (2013), by using a linear damage accumulation law, evaluated that the combined dynamic effects from winds and vehicles might result in serious fatigue problems for long-span bridges while, for the cable stayed bridge they considered as case study, the traffic or wind loads alone are not able to induce serious fatigue problems. Zhang *et al.*

*Corresponding author, Ph.D.
E-mail: francesco.petrini@uniroma1.it

 ISSN: 1225-4568 (Print), 1598-6217 (Online)

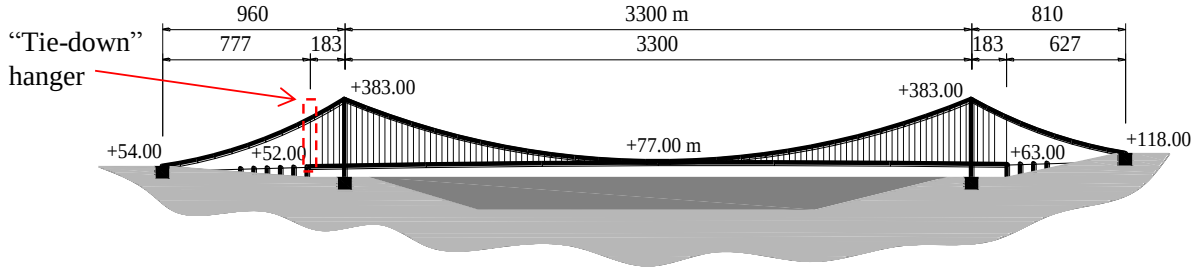

Fig. 1 Longitudinal scheme of considered bridge

(2014), conducted the fatigue life estimation of existing suspension bridge (three spans bridge with 154.8 m, 372.5 m, and 150.9 m lengths) under vehicle and hurricane (non-stationary) wind, concluding that the damage accumulation of the two actions can greatly affect the fatigue life. Cai *et al.* (2015), in a state of the art regarding coupled wind-vehicle-bridge system modeling, stated that the analysis of bridges under the combined actions of both wind and vehicles have been conducted only in a few studies so far, and possible fatigue damage due to the combined effect of loading from highway vehicles or railway trains and wind loading could accumulate.

In summary, previous studies seem to confirm the intuitive behavior where simultaneous wind-vehicle action has always a negative effect on the fatigue strength (fatigue damage due to the simultaneous action is greater than fatigue damage due to individual actions). In addition the fatigue damage accumulation due to the simultaneous action of wind and vehicle transit is often evaluated by the algebraic sum of the two contributions, also if for large suspension bridges it has been shown that, when wind is significant in intensity, the bridge vertical displacement response due to the presence of the moving vehicles can decrease (Chen and Cai 2007), and this behavior has been explained by interpreting the vehicle (if modeled as a system moving masses on springs) as a special tuned mass damper suppressing the vibration of the bridge (Chen and Wu 2008).

This research focuses on the evaluation of the fatigue damage in the hanger ropes of a long span suspension bridge (proposed Messina strait bridge, with 3300m long suspended span) due to the wind action and train transit, with particular focus on the interaction mechanisms between the two actions in terms of fatigue damage accumulation. The paper extends the investigations conducted for the same bridge in Petrini and Bontempi (2011), with the aim of clarifying the mechanisms behind the counterintuitive result obtained there: the fatigue damage accumulated during the simultaneous action of wind and train transit in some hanger ropes of the bridge can be lower that the algebraic sum of the two contributions evaluated separately, and it can be also lower than the fatigue damage due to the single action. Rational explanation of the phenomenon is provided on the evidence of some numerical results obtained from the time domain analyses carried-out by a complete three-dimensional finite element model of the bridge and by implementing well established and simplified models for wind and train induced forces, and for damage accumulation law. The main goal is not to propose novelties in modeling or theories used in dealing with the problem, rather the novelty is in the obtained results, which can be usefully commented to explain the above mentioned counterintuitive behavior, which is also not adequately studied in literature.

2. Case-study bridge and finite element modeling

Study is carried out on 4700 meters long suspension bridge open to both highway and railway traffic. The main span of the bridge is 3300 m long while the total length of the 60 meters wide deck is 3666 meters including the side spans. The deck is formed by three box sections; the outer ones support the roadways while the central one supports the railway. The roadway deck has three lanes for each carriageway (two driving lanes and one emergency lane) each 3.75 meters wide and the railway section has two tracks, with a symmetric in cross section (Petrini and Bontempi 2011). Suspension system of the bridge is formed by main cables and hanger ropes. There are three types of hanger ropes with different cross section: near the towers (cross sectional area A = 0,0327 m^2), mid span (A = 0,0137 m^2) and quarter span (A = 0,0117 m^2). Through the hanger ropes near the towers, those at both ends are called "tie-down" and have such as a particular and peculiar behavior, that could be considered as a different typology. The main task of the "tie-down" hangers is to stabilize the main cables of the support system, they are the most external vertical ropes and are positioned relatively far from the other hanger ropes, in addition they have a cross sectional area that is at least 1.5 times larger than other hangers (Sgambi *et al.* 2012).

A three dimensional finite element model of the bridge has been developed in the Ansys® code (http://www.ansys.com/) and shown in Fig. 2. Two nodes tridimensional beams with tension, compression, torsion and bending capabilities are adopted to model mono-dimensional elements for deck, piers and towers frame. The deck is formed by three lines of these elements whose assigned cross section properties reproduce geometry and stiffness of railway (central line) and highway (outer lines) girders. Integral behavior of the whole deck is ensured by transverse frames. The suspension system (main cables and hangers) is modeled with three-dimensional link elements, with a bilinear (elastic-plastic without hardening) stiffness, and having uniaxial tension-only behavior, also if elements

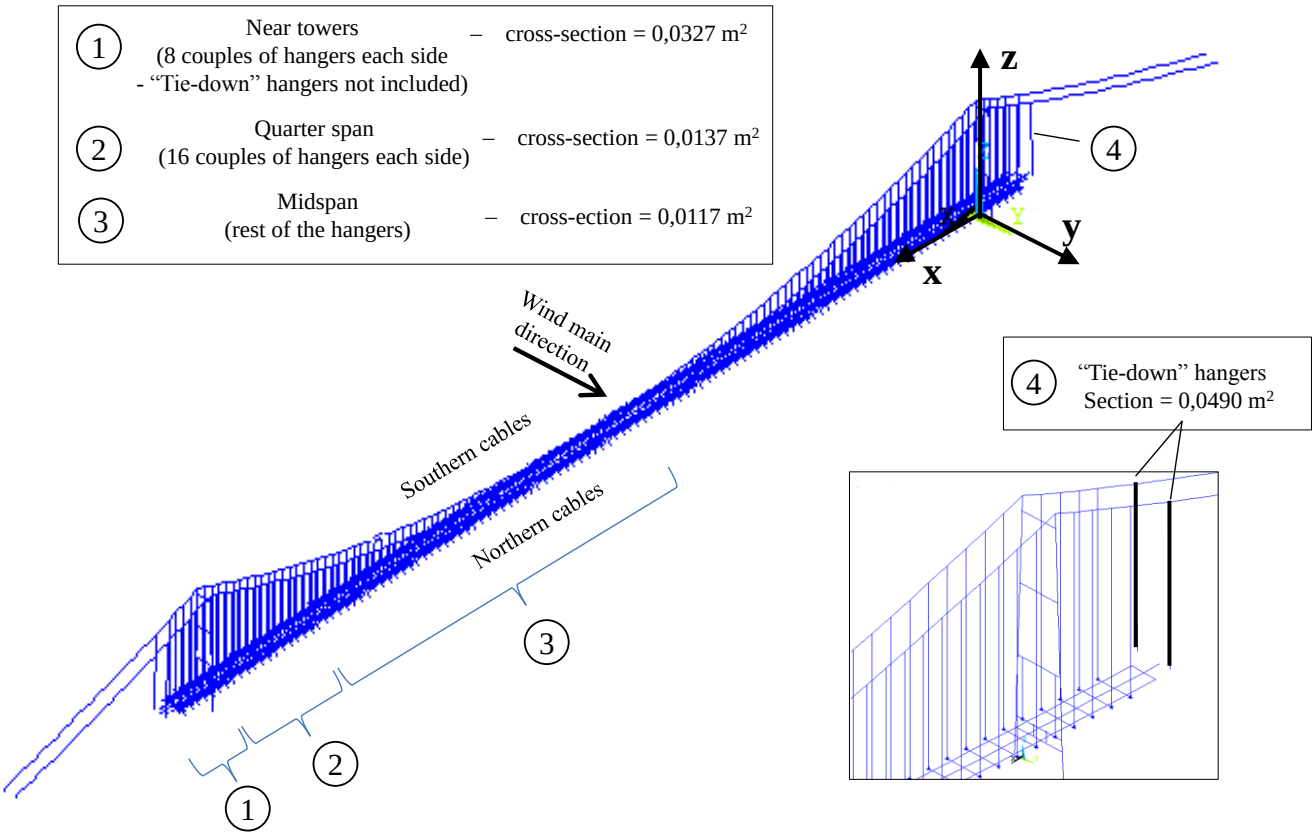

Fig. 2 3D-FE model of the bridge

remain in the elastic stress range. Punctual mass elements are adopted to reproduce structural masses of deck slab. Appropriate gap contact elements, which may maintain or break a contact and may slide relative to each other, are adopted to model damping devices that ensure a proper connection between deck and towers. Details on the connection between hanger ropes and the deck (realized without welded components) are provided in Petrini and Bontempi (2011). An implicit (modified Newton-Rapson) algorithm is used for solving the dynamical problem. It is worth noting that, due to the complexity of the structure, numerical errors can significantly affect the results obtained by non-tested models (Sgambi 2005), then the finite element model used here has passed a number of calibration tests carried out both by the current and other authors (Arangio *et al.* 2011).

3. Fatigue analysis

Fatigue analysis is performed in time domain using the so called S-N approach (Schijve 2004), the well-known technique of "rain flow counting method" RCM (Downing and Socie 1982) to reduce complex stress time histories into a set of simple equivalent stress reversals is also applied. Fatigue damage is evaluated with the Palmgren-Miner rule (Miner 1945) making the assumption of linear cumulative damage. This procedure has recognized limits, such as impossibility to consider effect of residual stress and of stress amplitudes under the fatigue limit of the considered

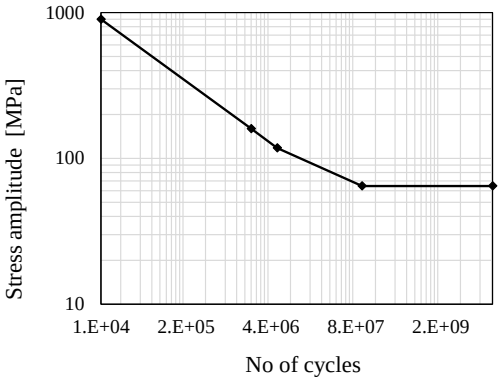

Fig. 3 Adopted S-N Curve

S-N curve, especially at notches. Another problem of a linear damage model is neglecting nonlinear phenomenon of macro plasticity accumulation (Huyen *et al.* 2008) that can led to crack nucleation. However, for sake of simplicity and since the goal of this paper is to clarify interaction effects between train and wind induced fatigue damage, the above mentioned approach is used despite all these limits.

Palmgren-Miner rule is the most common used damage model for fatigue analysis and it is recommended in several standards and codes, as for example EN 1993 (CEN 2003) and has been shown to be conservative with respect to the continuum damage mechanics approach (Li *et al.* 2002). The S-N curve selected for damage evaluation is the one with the greatest fatigue strength from EN 1993 referred to a detail category 160 N/mm² (Fig. 3).

This S-N curve is chosen for hanger ropes because fatigue problems can occur at the lower anchorages which are only axially loaded and, in such kind of structures, have a very high quality manufacture (e.g., there are not welded components), for details of the hanger socket attached to the deck plate refer to Petrini and Bontempi 2011.

In order to assess the effects of varying the mean stress, the modified Goodman relation (Schijve 2004) is used, by scaling the stress amplitudes calculated by the RCM

$$\frac{S_a}{[S_a]_{S_m=0}} = 1 - \left(\frac{S_m}{S_U}\right) \tag{1}$$

where S_a is the stress amplitude, S_m is the mean stress, $[S_a]_{Sm=0}$ is the equivalent fully reversed stress amplitude (by neglecting the mean value from S_a), and S_U is the ultimate tensile stress.

3.1 Wind and train load models

The overall wind speed is considered as the sum of mean and turbulent wind speed. The mean wind speed V_m is the average on a time interval of 10 minutes, it is characterized by long time variations, and it is considered as constant during the single wind event. The three-dimensional Cartesian coordinate system of the model is orientated in such way that the mean wind has a nonzero component along *y* only (that is orthogonal to the bridge deck, see Figure 2). Appropriate estimation of the fatigue life should accounts for the probabilistic distribution of wind direction (Xu *et al.* 2009), also if for the case-study bridge there is a strongly dominant wind blowing direction (see Fig. 4), its variability has been taken into account by appropriately projecting non-orthogonal wind time histories on the y-axis by considering an uniformly distributed random wind incidence angle between -15° and +15° with respect to the perfectly-orthogonal case.

The Power Spectral Density (PSD) matrix [*S*] characterizes completely the wind turbulent components *u*,*v*,*w*, assumed as a zero-mean Gaussian stochastic process (Simui and Scanlan 1996). The terms $S_{ijik}(n)$ (*i*= *u*,*v*,*w* and *j*,*k*=1,2,..,*N*) of $[S]_i$ are given by the well-established normalized half side Von Karman's power spectral density

$$\frac{nS_{ijij}(n)}{\sigma_i^2} = \frac{4n_i}{\left(1 + 70.8n_i^2(z)\right)^{\frac{5}{6}}} \tag{2}$$

$$S_{ijik}(n) = \sqrt{S_{ijij}(n)S_{ikik}(n)}\exp\left(-f_{jk}(n)\right) \tag{3}$$

where *n* is the current frequency (in Hz), *z* is the height (in m), σ_i^2 is the variance of the velocity fluctuations, $n_i(z)$ is a non-dimensional height dependent frequency and

$$f_{jk}(n) = \frac{|n|\sqrt{C_x^2\left(x_j - x_k\right)^2 + C_z^2\left(z_j - z_k\right)^2}}{\pi\left(V_m(z_j) + V_m(z_k)\right)} \tag{4}$$

where c_z and c_x represent the decay coefficients, which are inversely proportional to the spatial correlation of the wind velocity field (Di Paola 1998, Vassilopoulou *et al.* 2017), varying with mean wind intensity (Dimopoulos *et al.* 2016). Under these assumptions it results for the generic location (*j*) of wind forces application

$$V_x^{(j)} = u_j(t)\ ;\ V_y^{(j)} = V_{mj} + v_j(t)\ ;\ V_z^{(j)} = w_j(t) \tag{5}$$

Wind velocity time histories are digitally simulated with the weighted amplitude wave superposition method and proper orthogonal decomposition (POD) of the PSD matrix (Carassale and Solari 2006). A total of 74 wind velocity time histories are generated for each single simulated event (then *j*=1,2,..,74 in Eq. 5) in order to correctly take into account the wind field correlation along the bridge skyline, and they are applied along cables and deck. All the simulated wind time histories are 600 seconds long (plus an initial time window of 50 seconds, which is devoted to a ramp-type modulation function in intensity, inserted for numerical purposes).

Once wind velocity time-histories are generated, then the aerodynamic forces on bridge deck and cables are evaluated by the so-called Steady aeroelastic theory (Petrini *et al.* 2007). The drag (*D*), lift (*L*) and moment (*M*) instantaneous components of the aerodynamic forces are given by

$$D(t) = \frac{1}{2}\rho \cdot |V(t)|^2 * B * c_D[\gamma(t)] \tag{6}$$

$$L(t) = \frac{1}{2}\rho \cdot |V(t)|^2 * B * c_L[\gamma(t)] \tag{7}$$

$$M(t) = \frac{1}{2}\rho \cdot |V(t)|^2 * B^2 * c_M[\gamma(t)] \tag{8}$$

where ρ is the air mass density, $|V(t)|$ is the module of the wind instantaneous velocity evaluated as vector composition of the three components shown in Eq. (5), $\gamma(t)=\alpha(t)-\theta_0(t)$ with $\alpha(t)$ being the instantaneous angle of attack with respect to the horizontal plane of the wind velocity vector and θ_0 being the mean equilibrium position of the element under wind, *B* is a characteristic dimension of the cross section (*B*=deck width or cable diameter depending on the location of the application point of the force along the bridge), c_D is the aerodynamic drag coefficient. c_L and c_M are the aerodynamic lift and moment coefficients given by

$$c_L(\gamma) = c_L(\theta_0) + K_{L0}(\alpha - \theta_0) \tag{9}$$

$$c_M(\gamma) = c_M(\theta_0) + K_{M0}(\alpha - \theta_0) \tag{10}$$

where K_{L0} and K_{M0} are the angular coefficients of the $c_L(\gamma)$ and $c_M(\gamma)$ functions (experimentally derived and reported in Petrini and Bontempi 2011) computed in $\theta = \theta_0$.

Fatigue damage due to wind is evaluated referring to the time period of a year. A single wind mean speed cannot be representative of wind load on the bridge during a significant time period, such as a year, then a number of time-histories with different intensities of mean component are necessary. With the goal of reducing the computational costs, the fatigue damage for a windy day is evaluated by

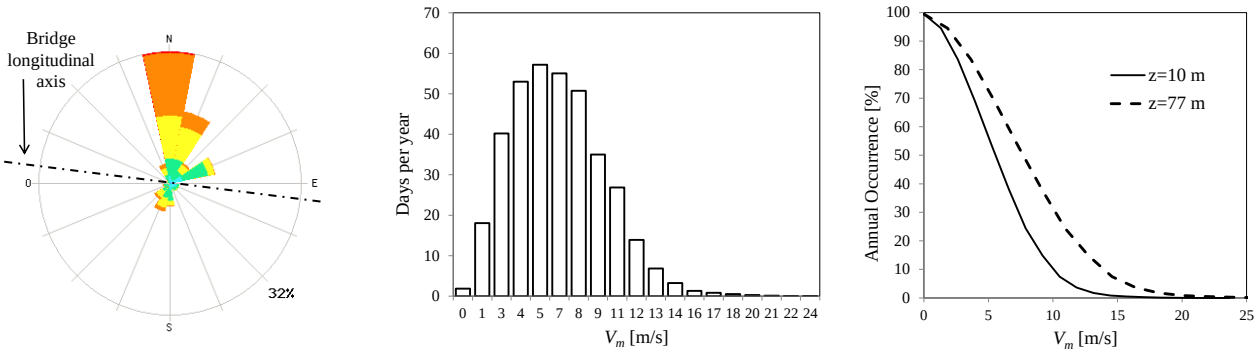

(a) wind directions (b) annual wind intensity (10 m height) (c) occurrence

Fig. 4 Time period 2010-2017 (after https://www.mareografico.it)

repeating continuously without any interruption, the 600sec wind time history for 12 hours. The annual fatigue damage is calculated in reference to conservative annual mean wind speed distribution, based on data recorded from The National Tidegauge Network (https://www.mareografico.it) during last seven years, shown in Table 1 and Fig. 4. Furthermore, the curve of annual frequency of exceeding of mean speed was modified according to the logarithmic law that describes how the mean velocity varies with height because the bridge deck is situated at 77 meters over the sea level and the wind speed are recorded at 10 meters

$$V(z) = \frac{u^*}{k} * \log_e\left(\frac{z}{z_0}\right) \tag{11}$$

In Eq. (11), u^* is the friction velocity, k is the von Karman constant and z_0 is the roughness length; u^* and k are determined from experimental data.

The assumptions made in evaluating the wind induced fatigue damage are summarized below

• 19 wind time histories groups (one group for each mean wind intensity shown in Table 1) are digitally simulated. Wind time histories have a duration of 600 seconds.

• Daily wind time histories are generated by repeating the single simulated event in order to obtain a 12 hours continuous wind event.

• Angle of incidence between -15° and +15° are randomly generated and used to evaluate the mean wind component orthogonally to the deck (y-axis in the model), while mean wind components on x and z axes are neglected.

Train has been modelled as a system of mobile forces with constant amplitude concentrated along the girder and moving at a constant speed always from Eastern side to Western side. This model implies the assumptions that dynamic interaction between train and bridge can be neglected and it is a reasonable hypothesis because of the small inertia of the vehicle in comparison with the mass of the structure. Train is modeled in reference to the LM 71 of the EN 1991 (CEN 2004). The considered train weights 8.8 ton/m and is 750 meters long transiting at velocity V_{tr}= 135 km/h (37,5 m/s). In order to evaluate fatigue damage due to train transit during a consistent time period of one year, it is also considered a transit every hour, for 18 hours a day, 6 days a week and 50 weeks a year. Therefore, the train load model is simplified as well because different train and vehicles could cross the bridge at the same time with different velocities, moving in the same or in the opposite direction at site-specific traffic characteristics (see e.g., Deng *et al.* 2018).

Bridge-train-wind interactions are not considered in terms of aerodynamics (presence of the train over the deck can alter the aerodynamic of the bridge) just to focus on the effects in terms of fatigue damage accumulation without adding uncertainties affecting the model of such a complex interaction (Chen and Wu 2008). Nevertheless, it is worth to note that, the aerodynamic interaction is expected to be not significant due to large value of the train/bridge size ratios.

Table 1 Assumed annual mean speed distribution

Mean wind speed (m/s)		Annual frequency (%)	Days (per year)
At 10 m height	At 77 m height		
0	0	0.00510	1.86
1	2	0.04941	18.03
3	4	0.11015	40.20
4	5	0.14520	53.00
5	7	0.15664	57.17
7	9	0.15087	55.07
8	11	0.13901	50.74
9	13	0.09588	35.00
11	15	0.07356	26.85
12	16	0.03811	13.91
13	18	0.01872	6.83
14	20	0.00892	3.26
16	22	0.00363	1.33
17	24	0.00231	0.84
18	26	0.00139	0.51
21	29	0.00029	0.11
22	31	0.00009	0.03
24	33	1.18E-05	4.30E-03

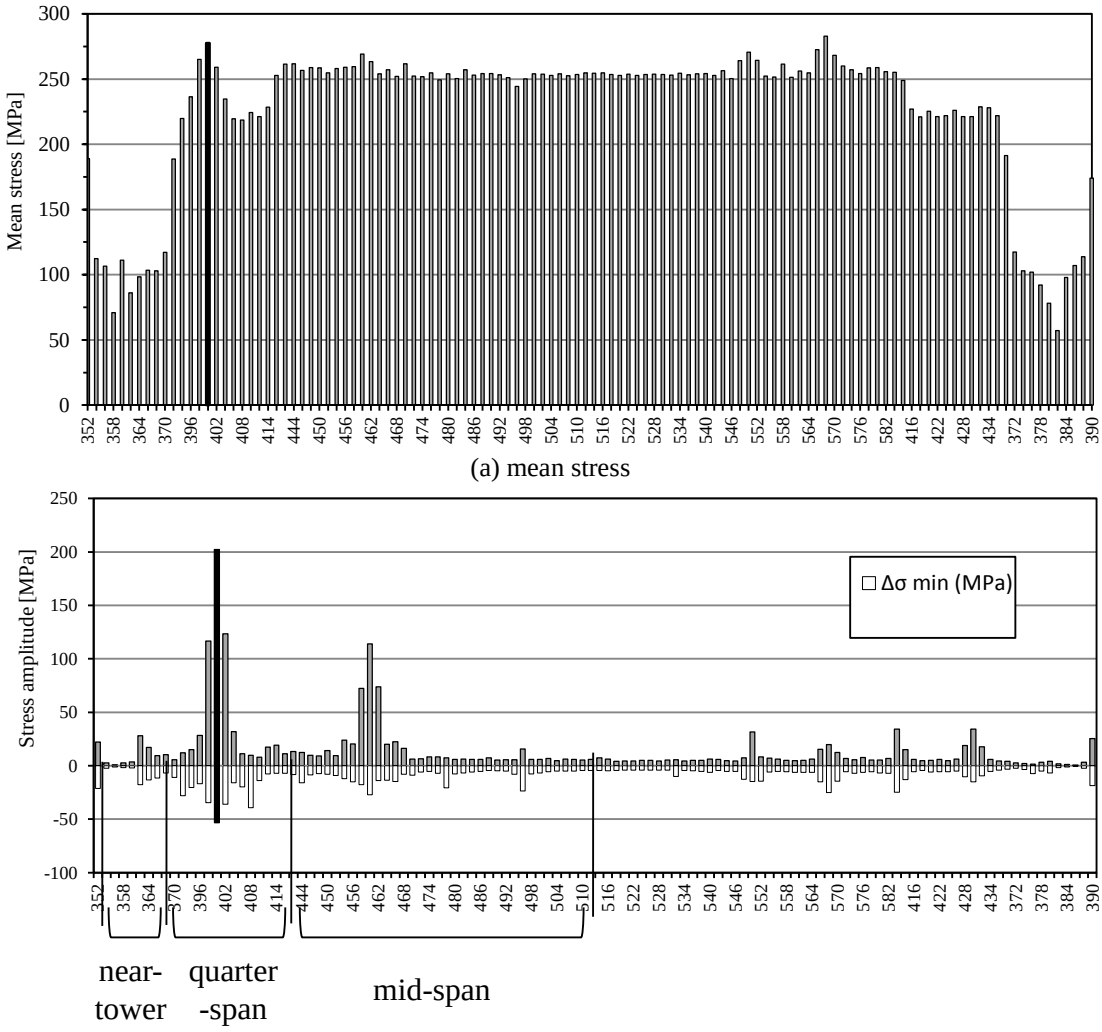

(a) mean stress

(b) maximum and minimum deviation from mean stress

Fig. 5 Fatigue proneness for northern hangers under wind action (V_m=15 m/s) and individuation of critical cables (in bold black). The x-axis in figure indicates the cable/hanger number

4. Annual fatigue damage evaluation under wind or train transit

In order to find the fatigue prone hanger ropes preliminary analyses were performed under wind loading (V_m=15 m/s at the deck height) or a train transit (V_{tr}=80 km/h). For both analyses the stress time histories in all hanger ropes were classified in terms of two stress fatigue proneness-revealing parameters evaluated during load cycle (see Fig. 5): (i) mean value, (ii) maximum and minimum deviation from mean value.

According to the above described fatigue indexes, vulnerability of hanger ropes to wind forces and train transit are identified and shown in Table 2 and Fig. 6.

Fatigue damage evaluation for all vulnerable hanger ropes is performed according with all previously described assumptions. A safety coefficient γ_F=1.35 was adopted in increasing the value of the stress amplitudes derived by the RCM. The annual fatigue damage due to wind ($D_{w,year}$) has been estimated for the hanger ropes by conducting time histories analyses under wind at different intensities (mean wind speed) shown in Table 1 and then multiplying the single-event (daily) damage by the number of days associated to that wind speed (Table 1). The annual fatigue damage due to train transit ($D_{tr,year}$) has been estimated by multiplying the damage due to the single train transit by the numbers of trains estimated to cross the bridge during the year (see section 3.1). The computed annual damages are shown in Fig. 7.

Concerning $D_{w,year,}$ there is no weakness accumulation in most of the hanger ropes till wind mean speed reaches about 18 m/s at the deck height, this is because induced stress amplitudes are under the fatigue limit identified by the S-N curve shown in Fig. 3. Only for identified wind critical cables in quarter span (399, 400-critical under wind forces) and mid span (460, 567) damage accumulation occurs for lower intensities of the wind speed (starting from 7 m/s).

Fatigue damage $D_{tr,year}$ has a more homogeneous distribution through the considered hanger ropes, with elements near towers being less prone to fatigue problems, extreme case is represented by Northern cable 362 which

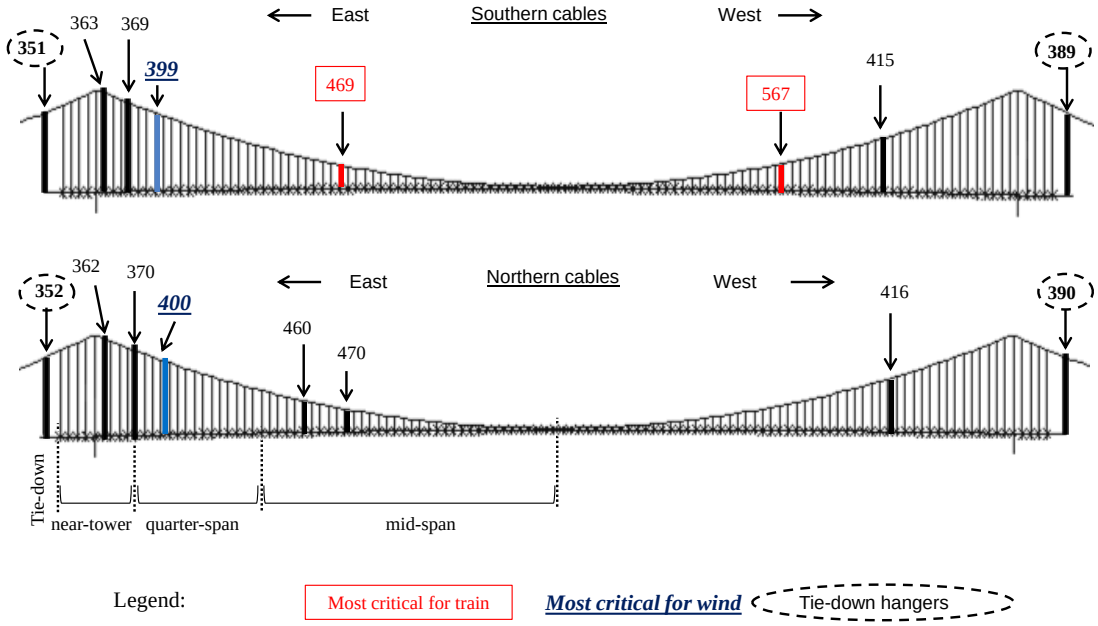

Fig. 6 Hangers which are vulnerable to fatigue damage and individuation of most critical hangers for wind action and train transit

does not suffer any D_{Tr} fatigue damage, meaning that the fatigue limit is not exceeded by maximum stress amplitudes induced by the train transit.

It is worth to highlights that the bridge is not fully symmetric: the west and east sides differ in many aspects (some of them are indicated in Fig. 1) like deck height, position of main cable anchorages with respect to towers, relative height between tower top and deck and many others. Consequently, the most vulnerable cables to fatigue are not in symmetric positions with respect to the mid-span.

Regarding the difference between cables 362 and 363 (located in the same abscissa along the deck but on opposite sides of the deck section), it is due to the fact that, since the wind is applied mainly from the south toward the north side, as indicated in Fig. 4, the average tension stress in hanger No 362 is higher than in the 363 due to their different deformation: hanger 362 is (in average) more elongated than 363 due to the rotation of the deck which under wind action is (in average) not equal to zero.

Furthermore, due to the large size of the bridge, each hanger is located 30 m far away from the successive on the same (northern or southern) side. Then hangers No 363 and 369, for example, are 90 m faraway each other, which makes a certain difference between the wind action "felt" by the hangers. Moreover, hanger No 363 is the nearest to the bridge tower, and its internal stress is conditioned by the larger local stiffness of the structure in this location with respect to the rest of the bridge, the local stiffness at the location of the hanger 369 is considerably lower.

Table 2 Summary of fatigue critical cables

Cable No	Position	Critical for
351 (tie-down)	Near Tower (East side)	Train
352 (tie-down)	Near Tower (East side)	Train
389 (tie-down)	Near Tower (West side)	Train
390 (tie-down)	Near Tower (West side)	Train
362	Near Towers (East side)	Wind
363	Near Towers (East side)	Train
369	Near Towers (East side)	Train
370	Near Towers (East side)	Train
399	Quarter span (East side)	Wind (most critical)
400	Quarter span (East side)	Wind (most critical)
415	Quarter span (West side)	Train
416	Quarter span (West side)	Train
460	Mid span (East side)	Train
469	Mid span (West side)	Train (most critical)
470	Mid span (East side)	Train
567	Mid span (West side)	Train (most critical)

5. Wind-train interaction effect on fatigue damage accumulation in hanger ropes

To investigate the coupling effects of wind load and train transit in terms of fatigue damage accumulation, a first comparison is made in Fig. 8 between fatigue damage evaluated from i) stress time-histories related to simultaneous wind blowing and train traffic (D_{tr+w}) and ii) the algebraic sum of previous analyses under individual actions ($D_{tr}+D_w$). To this regard analyses results reveal that

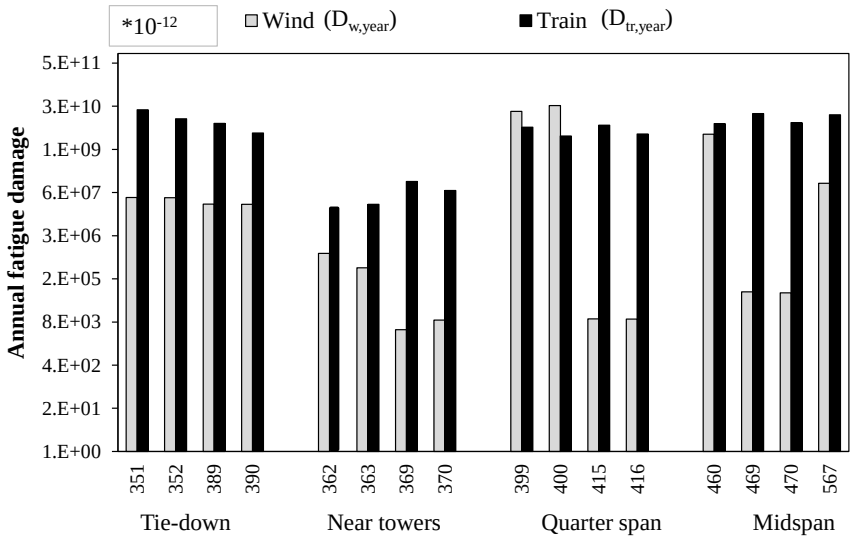

Fig. 7 Annual fatigue damage in hanger ropes due to the individual actions. The x-axis in figure indicates the cable/hanger number. The y-axis in in Log-scale

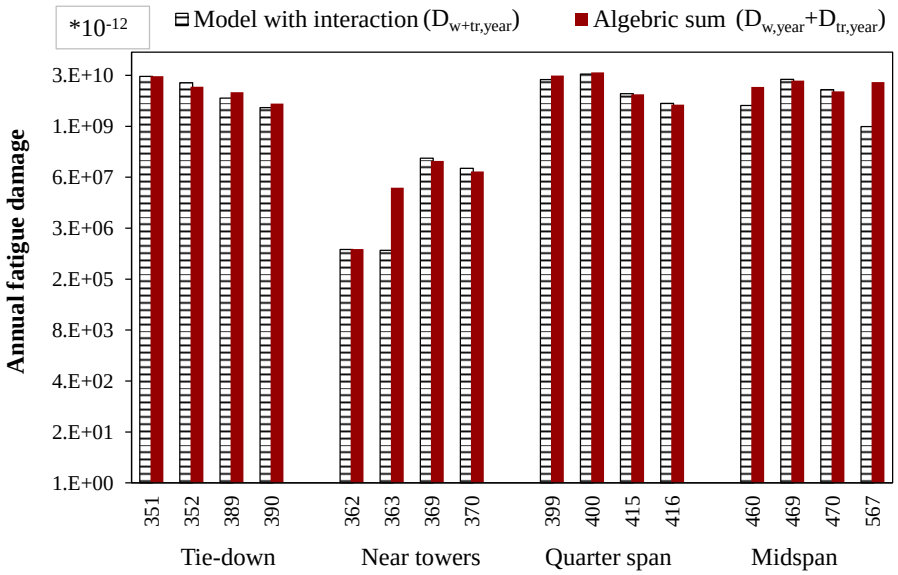

Fig. 8 Comparison between annual fatigue damage evaluated as: algebraic sum of separated actions contribution or from simultaneous action model. The x-axis in figure indicates the cable/hanger number. The y-axis in in Log-scale

all hanger ropes for which wind-induced annual fatigue damage $D_{w,year}$ is less than a certain level (hangers 369, 370, 415, 416, 469, 470), it results $D_{tr+w,year}>D_{tr,year}+D_{w,year}$, meaning that considering the train-wind fatigue interaction leads to an increasing of the computed fatigue damage, then in these cases it is not conservative to assume different loads acting separately. Results on some other hangers (e.g., 399, 400, 460) shown that estimating the damage as $D_{tr,year}+D_{w,year}$ it is conservative, but the difference with $D_{tr+w,year}$ is considerable in some cases (e.g., hangers 363 and 567).

The differences in terms of fatigue damage accumulated in hangers due to different accumulation mechanisms in case of wind-train interaction is shown in Fig. 9, where a comparison is made between D_{tr+w} and the damage evaluated by stress time-histories related to separate actions of wind action and train traffic (D_w and D_{tr} respectively). The comparison in Fig. 9 highlights the counterintuitive result anticipated above: it can been seen that there are some cases where $D_{tr+w,year}<D_{tr,year}$ and/or $D_{w,year}$ (hanger 363 at near towers and hangers 460, 567 at mid span).

To investigate further the described result, stress time histories associated with different fatigue behaviors are shown and discussed in what follow: hanger ropes number 363 (near towers hager with $D_{tr+w} < D_{tr}+D_w$ and $D_{tr+w} < D_{tr}$) and 369 (near towers hanger with $D_{tr+w}>D_{tr}+D_w$) are considered under the simultaneous action of wind and train at different wind intensities. In addition, also the "Tie-Down" cable 352 ($D_{tr+w} > D_{tr}+D_w$) is considered because this hanger ropes family has a peculiar behavior.

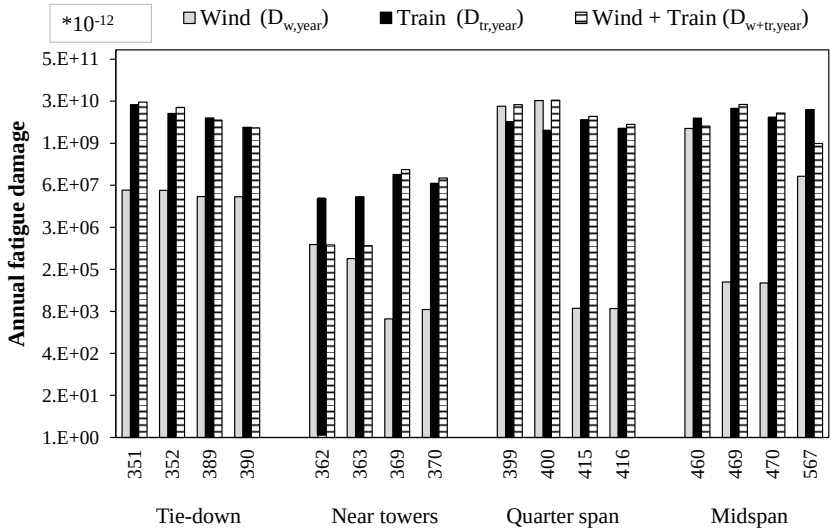

Fig. 9 Comparison between fatigue damage evaluated by separated analysis and that evaluated from simultaneous action model. The x-axis in figure indicates the cable/hanger number. The y-axis in in Log-scale

Furthermore, these cables are chosen because their stress time histories are appropriate to highlight interesting interaction aspects which are of general validity.

Fig. 10 shows that the main effect of wind forces at different wind intensity on cable 363 is a relevant increasing of mean stress value compared to the self-weight induced stress (difference between the stationary parts of the mean stress either in presence or in absence of wind). Due to the non-linear behavior of the structure (increasing cables deflection resulting in an increasing stiffness), this mean stress state variation results is a lower oscillation generated by the train transit than the same generated in the structure without wind.

For cable 369, where $D_{tr+w} > D_{tr}+D_w$ (see Fig. 11), the presence of wind forces does not relevantly affect the stress state induced by self-weight, with the superimposition of low amplitude stress oscillations that does not increase significantly the mean value of stress and also the stress variation due to train traffic remains the same, but the variance of the time history in general increases, resulting in an increasing of the accumulated damage. Furthermore when wind intensity is 30 m/s the cable experiences relevant oscillations that slightly reduce the mean stress state.

Hanger rope 352 (see Fig. 12), such as other "tie-down" cables, experiences large vibrations (due to a slightly-damped resonance of the main cable portion positioned outer to the tower, where the hanger is located) immediately after train transit and when the train is still on the bridge, something that is not observed in other hanger ropes. However also in this case, the presence of the wind load increases the mean value of stress with a reduction of excursion due to train traffic. This effect is less evident than in previous discussed hanger 363 and in other cables also because wind induced oscillations have relevant amplitudes and show a significant superimposition with the above-mentioned resonance effect (see for example Fig. 12(d)).

From the results shown above it can be argued that wind-train interaction mechanisms have a great relevance in fatigue damage evaluation because of the non-linear behavior that is typical of the considered structural typology. According to the standard assessment procedure (used here) for cycle counting and damage accumulation assumptions, and on the basis provided by the presented results, the following fundamental interaction behaviors can be identified:

- cables for which $D_{tr+w} < D_{tr}+D_w$ are those in which wind load increases the mean stress reducing the excursion due to train traffic thus fatigue damage evaluated as algebraic sum gives a higher value of the fatigue damage obtained by numerical analyses conducted considering simultaneous actions of wind and train because the variation of the mean stress effect is neglected. This result is due to the nonlinear behavior of the suspension bridge system and of the hanger ropes whose stiffness increases with deflections (that is when the stress state increases);
- in cables where $D_{tr+w}>D_{tr}+D_w$, wind load produces additional oscillations that superimpose to the train-induced ones without significantly altering the stiffness of the hanger. This superimposition then lead to additional fatigue damage accumulation because the resulting stress time histories increase in variance (with larger stress peaks); therefore stress amplitudes evaluated by the RCM are greater than those obtained in case of individual actions;
- "tie-Down" hanger ropes have a peculiar behavior because even if wind forces increase the mean stress value, the consequent reduction of train transit effect is not crucial as in other cables. In fact, the increasing of the mean stiffness of the bridge system due to the wind-induced deformation it is not necessary sufficient to make $D_{tr+w}<D_{tr}+D_w$. This is because there is a relevant stress fluctuation due to the previously mentioned resonance effect after train transit that strongly affect damage evaluation and cannot be considered when separated loadings analyses were performed.

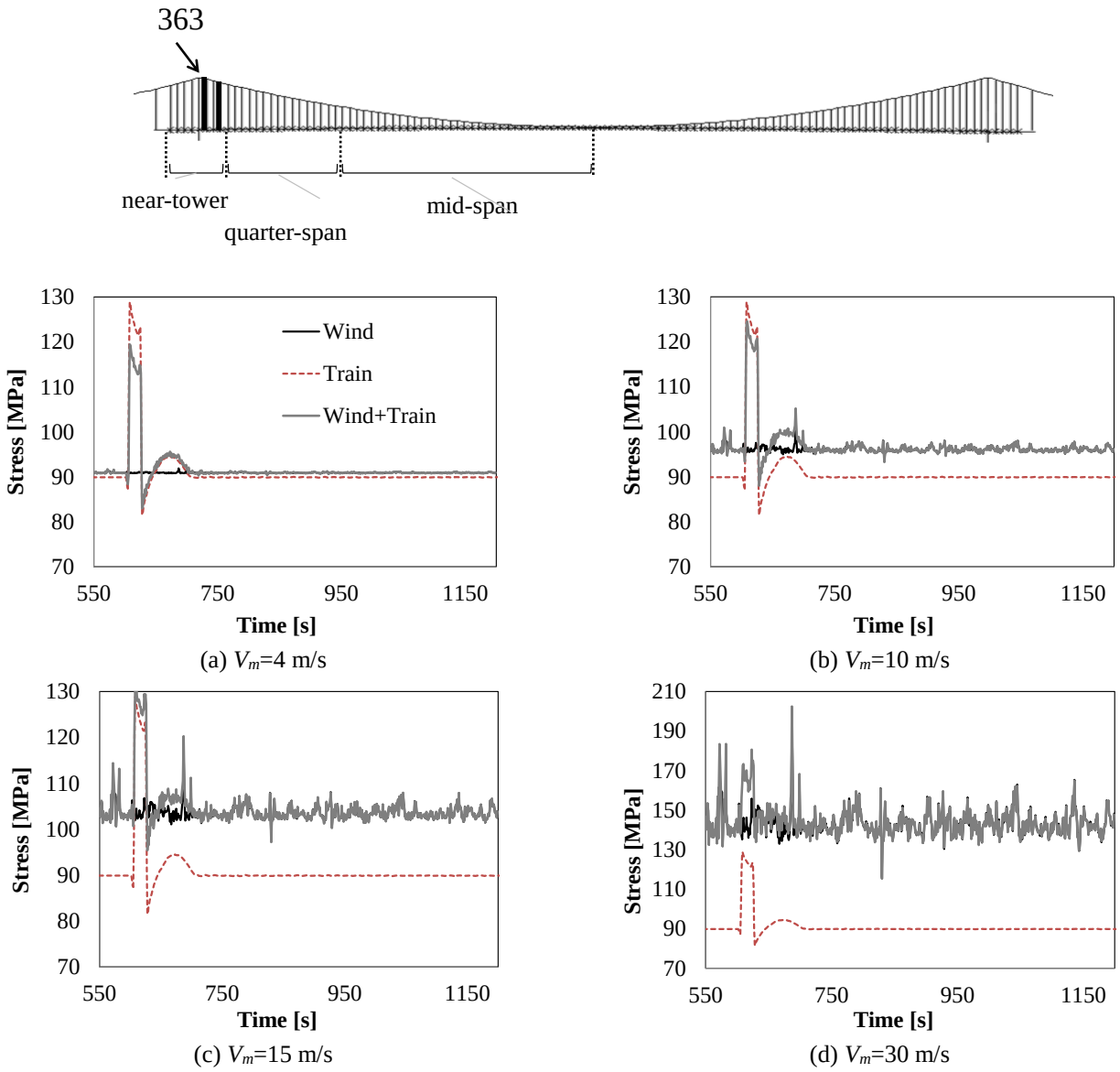

Fig. 10 Stress time-histories in cable 363 (D_{tr+w}<D_{tr}+D_w) for different wind mean speeds

6. Conclusions

A fatigue analysis of hanger ropes belonging to a long suspension bridge under wind load and train traffic has been carried out. In particular the effect of loading interaction mechanisms on the fatigue damages of hanger ropes have been investigated in detail. Analysis have been conducted in time domain using the "rain flow counting" method to evaluate stress amplitudes from stress time histories and the evaluation of the fatigue damage has been assessed using the "Palmgren-Miner" rule. Analyses have been carried out to find cables prone to fatigue failure for both wind load and train traffic. The adopted procedure is a simplified fatigue proneness analysis based on classification of the stress time histories in terms of two fatigue sensibility revealing parameters. Then, annual fatigue damage has been evaluated.

Principal results are:

• Train traffic induced fatigue damages have a more homogeneous distribution among all cables than wind induced fatigue damages.

• Train traffic produces large fatigue damage than wind load in hanger ropes. The wind load has relevance for fatigue damage only for critical hangers and for large wind intensities; these elements should be identified in the design of the suspension bridge.

• In hanger ropes for which the mean stress state is not affected by wind load, the simultaneous occurrence of wind load and train traffic produces a greater fatigue damage than the one evaluated as algebraic sum of damages from separated action of considered loadings ($D_{tr+w} > D_{tr}+D_w$).

• In hangers for which the mean stress state depends on wind intensity (mean wind speed), the damage evaluated as algebraic sum of separated analyses is larger than the one computed from stress time history due to simultaneous loads ($D_{tr+w} < D_{tr}+D_w$). This result is due to the non-linear stiffness behavior of the structure, causing lower train induced stress amplitudes at increasing mean stress values.

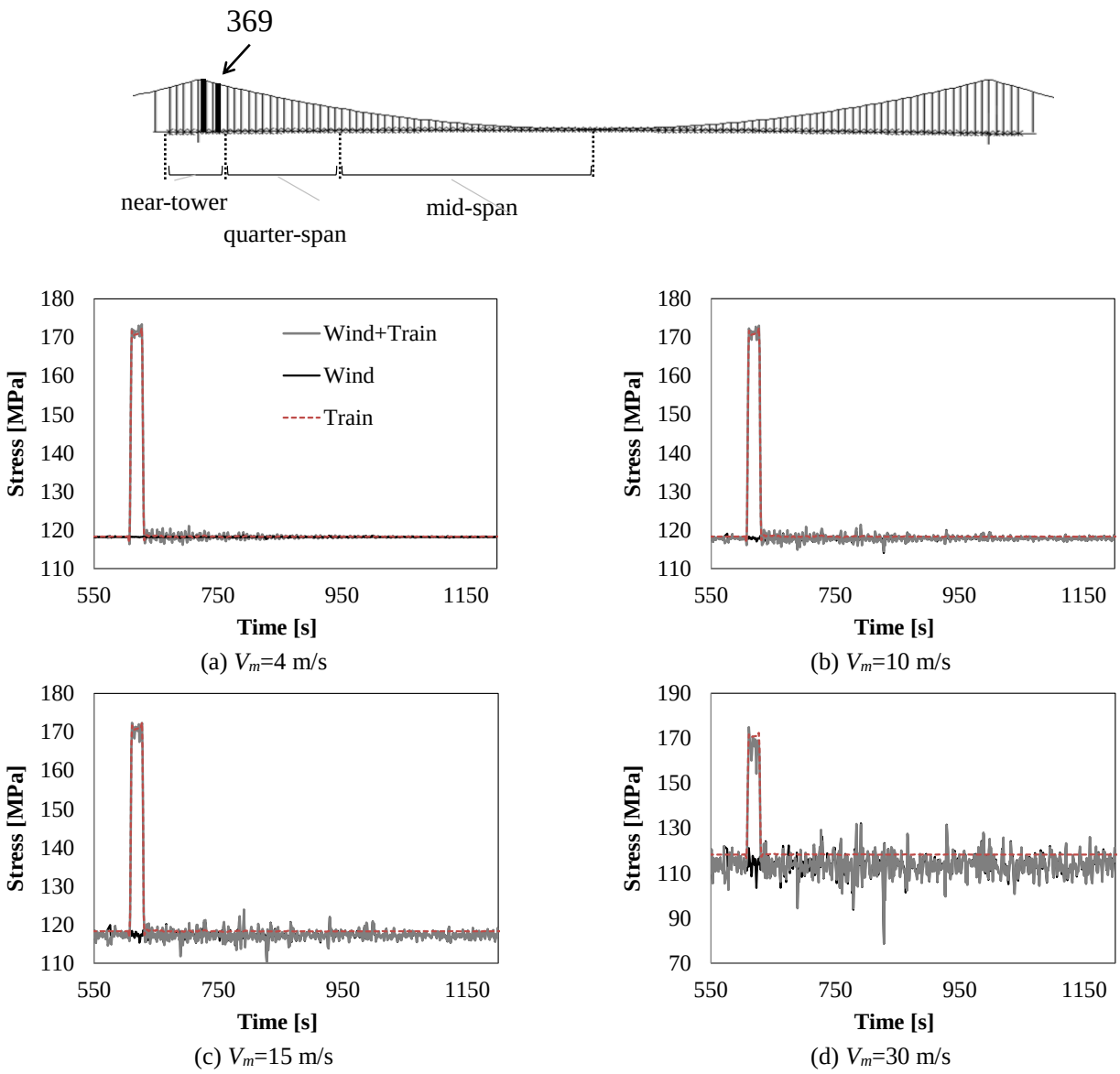

Fig. 11 Stress time-histories in cable 369 (D_{tr+w}>D_{tr}+D_w) for different wind mean speeds

In these cases, if the damage is evaluated by algebraic sum of individual contributions, the fatigue strength can be largely underestimated.

• "Tie-down" cables are critical for both wind and train traffic loads and have a specific behavior in terms of experienced stress time history. The wind-train interaction results in a superposition of wind-induced vibrations to already present large oscillations caused by a resonance effect between the main cable and the external forces.

All the above considerations allow the rational understanding of the counterintuitive behavior observed in a previous author's paper (and not reported other where in the literature) and shown in Figure 9: if standard methods are adopted for stress-cycle counting and fatigue damage accumulation, the simultaneous action of wind load and train transit can lead to a fatigue damage in hangers that is less of the one induced by single actions.

Some useful design considerations for this kind of bridges can be obtained from the above mentioned results, for example, a higher number of "tie-down" hangers (outside the main span) could help to mitigate the effect shown in Fig. 12, but they essentially cannot eliminate it. The reason for this is that the "outer" part of the main suspension cable suffers large response to the dynamic loads due to the presence of the fixed point at the top of the tower, which also causes the inversion of the curvature of its deformed shape with respect to the inner part. These circumstances together with the values of the eigen frequencies associated with higher mode shapes involving locally the outer part of the main cable, are able to produce these large oscillations. The appropriate number of additional "tie-down" hangers that should be installed for mitigating this effect is not easy to be quantified and has to be evaluated by appropriate parametric analyses, which are out of the scope of this paper.

Since the outlined behaviors are mainly due to the geometric non-linearity of such a kind of structures (suspension bridges), the main message/conclusions (the

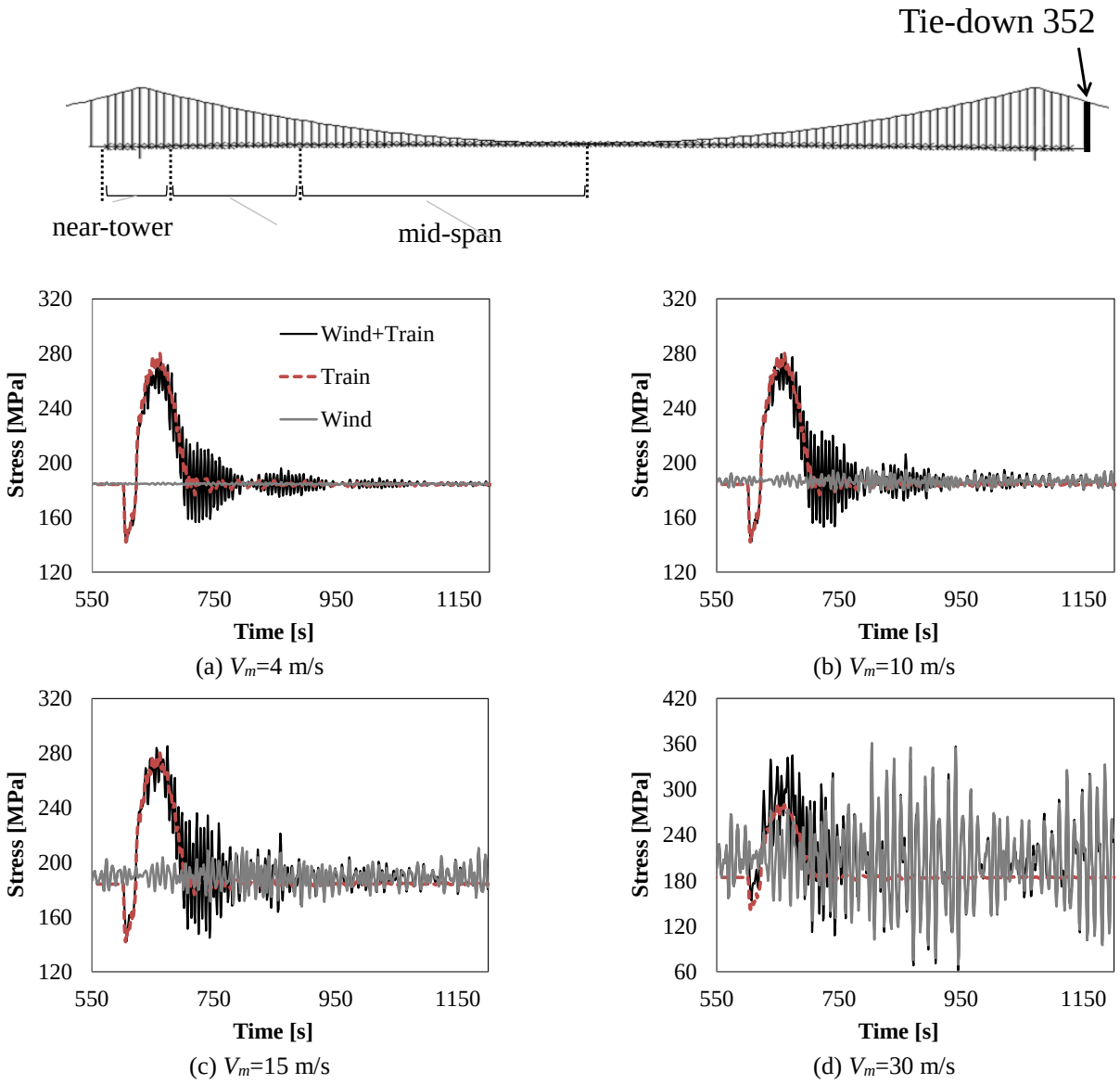

Fig. 12 Stress time histories in "Tie-down" cable 352 for different wind mean speeds

fatigue behavior of cables can be "counterintuitive" or as not as expected on the basis of simplistic analyses which do not consider wind-train coupling effects) have general validity for suspension bridges. Of course to what extent these "counterintuitive" behaviors can affect the bridge design it depends on the specific bridge features (e.g., span of the bridge)

Further developments will be devoted to the refinement of the assumptions made in this paper concerning the train traffic (more than one train will be considered to cross the bridge at the same time) and the aerodynamics of the system (the alteration of the bridge aerodynamic due to the presence of the train will be considered).

Acknowledgments

The authors would like to acknowledge Mr. Roberto Raddi, which is past MSc student at Sapienza University of Rome (part of the results and comments contained in this work have been inserted in his MSc dissertation, discussed on May 2014) for the fruitful discussion related with the paper.

References

Arangio, S., Bontempi, F. and Ciampoli, M. (2011), "Structural integrity monitoring for dependability", *Struct. Infrastruct. Eng.-Mainten. Manage. Life-Cycle Des. Perform.*, **7**(1-2), 75-86. https://doi.org/10.1080/15732471003588387.

Barbato, M., Palmeri, A. and Petrini, F. (2014), "Special issue on performance-based engineering", *Eng. Struct.*, **78**, 1-2.

Brando, F., Cao, L., Olmati, P. and Gkoumas, K. (2012), "Consequence-based robustness assessment of bridge structures", *Proceedings of the 6th International Conference on Bridge Maintenance, Safety and Management*, Stresa, Lake Maggiore, Italy, July.

Cai, C.S., Hu, J., Chen, S., Han, Y., Zhang, W. and Kong, X.

(2015), "A coupled wind-vehicle-bridge system and its applications: A review", *Wind Struct.*, **20**(2), 117-142. http://dx.doi.org/10.12989/was.2015.20.2.117.

Carassale, L. and Solari, G. (2006), "Montecarlo simulation of wind velocity field on complex structures", *J. Wind Eng. Industr. Aerodyn.*, **94**(5), 323-339. https://doi.org/10.1016/j.jweia.2006.01.004.

CEN-European Committee for Standardization (2003), *EN 1993-1-9: Design of Steel Structures - Part 1-9: Fatigue Strength of Steel Structures*, Brussels, Belgium.

CEN- European Committee for Standardization (2004), *EN 1991-1-4: Actions on Structures*, Brussels, Belgium.

Chan, T.H.T., Guo, L. and Li, Z.X. (2003), "Finite element modelling for fatigue stress analysis of large suspension bridges", *J. Sound Vibr.*, **261**(3), 443-464. https://doi.org/10.1016/S0022-460X(02)01086-6.

Chan, T.H.T., Zhou, T.Q., Li, Z.X. and Guo, L. (2005), "Hot spot stress approach for Tsing Ma Bridge fatigue evaluation under traffic using finite element method", *Struct. Eng. Mech.*, **19**(3), 1-19. https://10.12989/sem.2005.19.3.261.

Chen, S.R. and Cai, C.S. (2007), "Equivalent wheel load approach for slender cable-stayed bridge fatigue assessment under traffic and wind: Feasibility study", *J. Brid. Eng.*, **12**(6), 755-764. https://doi.org/10.1061/(ASCE)1084-0702(2007)12:6(755).

Chen, S.R. and Wu, J. (2008), "Performance enhancement of bridge infrastructure systems: Long-span bridge, moving trucks and wind with tuned mass dampers", *Eng. Struct.*, **30**(11), 3316-3324. https://doi.org/10.1016/j.engstruct.2008.04.035.

Chen, Z.W., Xu, Y.L., Li, Q. and Wu, D.J. (2011), "Dynamic stress analysis of long suspension bridges under wind, railway, and highway loadings", *J. Brid. Eng.*, **16**(3), 383-391. https://doi.org/10.1061/(ASCE)BE.1943-5592.0000216.

Di Paola, M. (1998), "Digital simulation of wind field velocity", *J. Wind Eng. Industr. Aerodyn.*, **74**, 91-109. https://doi.org/10.1016/S0167-6105(98)00008-7.

Dimopoulos, C.A., Koulatsou, K., Petrini, F. And Gantes, C.J. (2015), "Assessment of stiffening type of the cutout in tubular wind turbine towers under artificial dynamic wind actions", *J. Comput. Nonlin. Dyn*, **10**(4), 041004. https:// 10.1115/1.4028074.

Deng, Y., Li, A. and Feng, D. (2018), "Fatigue performance investigation for hangers of suspension bridges based on site-specific vehicle loads", *Struct. Health Monitor.*, 1475921718786710. https://doi.org/10.1177/1475921718786710.

Downing, S.D. and Socie, D.F. (1982), "Simple rainflow counting algorithms", *Int. J. Fatig.*, **4**(1), 31-40. https://doi.org/10.1016/0142-1123(82)90018-4.

Gimsing, N.J. and Georgakis, C.T. (2012), *Cable Supported Bridges: Concept and Design*, 3rd Edition, John Wiley & Sons Inc., New York, U.S.A.

Huyen, N., Flaceliere, L. and Morel, F. (2008), "A critical plane fatigue model with coupled meso-plasticity and damage", *Fatig. Fract. Eng. Mater. Struct.*, **31**(1), 12-28. https://doi.org/10.1111/j.1460-2695.2007.01197.x.

Klinger, C., Michael, T. and Bettge, D. (2014), "Fatigue cracks in railway bridge hangers due to wind induced vibrations-failure analysis, measures and remaining service life estimation", *Eng. Fail. Analy.*, **43**, 232-252. https://doi.org/10.1016/j.engfailanal.2014.02.019.

Li, Z.X., Chan, T.H.T. and Ko, J.M. (2002), "Evaluation of typhoon induced fatigue damage for Tsing Ma bridge", *Eng. Struct.*, **24**(8), 1035-1047. https://doi.org/10.1016/S0141-0296(02)00031-7.

Liu, Z., Guo, T., Huang, L. and Pan, Z. (2017), "Fatigue life evaluation on short suspenders of long-span suspension Bridge with central clamps", *J. Brid. Eng.*, **22**(10), 04017074. https://doi.org/10.1061/(ASCE)BE.1943-5592.0001097.

Manenti, S. and Petrini, F. (2010), "Dynamic analysis of an offshore wind turbine: Wind-waves nonlinear interaction. *Proceedings of the 12th International Conference on Engineering, Science, Construction, and Operations in Challenging Environments-Earth and Space 2010*, Honolulu, Hawaii, U.S.A., March.

Miner, M.A. (1945), "Cumulative damage in fatigue", *J. Appl. Mech.*, **67**, A159-4.

Olmati, P. and Giuliani, L. (2013), "Progressive collapse susceptibility of a long span suspension bridge", *Proceedings of the 2013 Structures Congress*, Pittsburgh, Pennsylvania, U.S.A., May.

Olmati, P., Gkoumas, K., Brando, F. and Cao, L. (2013), "Consequence-based robustness assessment of a steel truss bridge", *Steel Compos. Struct.*, **14**(4), 379-395. https://10.12989/scs.2013.14.4.379.

Petrini, F. and Bontempi, F. (2011), "Estimation of fatigue life for long span suspension bridge hangers under wind action and train transit", *Struct. Infrastruct. Eng.-Mainten. Manage. Life-Cycle Des. Perform.*, **7**(7-8), 491-507. https://doi.org/10.1080/15732479.2010.493336.

Petrini, F., Giuliano, F. and Bontempi, F, (2007), "Comparison of time domain techniques for the evaluation of the response and the stability of long span suspension bridges", *Comput. Struct.*, **85**(11-14), 1032-1048. https://doi.org/10.1016/j.compstruc.2006.11.015.

Schijve, J. (2004), *Fatigue of Structures and Materials*, Kluwer Academic Publishers, Norwell, Massachusetts, U.S.A.

Sgambi, L. (2005), "Handling model approximations and human factors in complex structure analyses", *Proceedings of the 10th International Conference on Civil, Structural and Environmental Engineering Computing*, Rome, September.

Sgambi, L., Gkoumas, K. and Bontempi, F. (2012), "Genetic algorithms for the dependability assurance in the design of a long-span suspension bridge", *Comput.-Aid. Civil Infrastruct. Eng.*, **27**(9), 655-675. https://doi.org/10.1111/j.1467-8667.2012.00780.x.

Sgambi, L., Garavaglia, E., Basso, N. and Bontempi, F. (2014), "Monte Carlo simulation for seismic analysis of a long span suspension bridge", *Eng. Struct.*, **78**, 100-111. https://doi.org/10.1016/j.engstruct.2014.08.051.

Simiu, E. and Scanlan, R.H. (1996), *Wind Effects on Structures*, 3rd Edition, John Wiley & Sons Inc., New York, U.S.A.

Sun, Z., Ning, S. and Shen, Y. (2017), "Failure investigation and replacement implementation of short suspenders in a suspension bridge", *J. Brid. Eng.*, **22**(8), 05017007-1-9. https://doi.org/10.1061/(ASCE)BE.1943-5592.0001089.

Xu, Y.L., Liu, T.T. and Zhang, W.S. (2009), "Buffeting-induced fatigue damage assessment of a long suspension bridge", *Int. J. Fatig.*, **31**(3), 575–586. https://doi.org/10.1016/j.ijfatigue.2008.03.031.

Ye, X.W., Su, Y.H. and Han, J.P. (2014) "A state-of-the-art review on fatigue life assessment of steel bridges", *Math. Probl. Eng.* http://dx.doi.org/10.1155/2014/956473.

Vassilopoulou, I., Petrini, F. and Gantes, C.J. (2017). "Nonlinear dynamic behavior of cable nets subjected to wind loading", *Struct.*, **10**, 170-183. https://doi.org/10.1016/j.istruc.2017.03.004.

Zhang, W., Cai C.S. and Pan, F. (2013), "Fatigue reliability assessment for long-span bridges under combined dynamic loads from wind and vehicles", *J. Brid. Eng.*, **18**(8), 735-747. https://doi.org/10.1061/(ASCE)BE.1943-5592.0000411.

Zhang, W., Cai, C.S., Pan, F. and Zhang, Y. (2014), "Fatigue life estimation of existing bridges under vehicle and non-stationary hurricane wind", *J. Wind Eng. Ind. Aerodyn.*, **133**, 135-145. https://doi.org/10.1016/j.jweia.2014.06.008.

Zhong, W., Ding, Y.l., Song, Y.S. and Zhao, H.W. (2018), "Fatigue behavior evaluation of full-field hangers in a rigid tied arch high-speed railway bridge: Case study", *J. Brid. Eng.*, **23**(5), 05018003-1-05018003-13. https://doi.org/10.1061/(ASCE)BE.1943-5592.0001235.

CC